JOURNAL OF MATERIALS SCIENCE **33** (1998) 4953–4960

A new model for the transverse modulus of unidirectional fiber composites

SHAO-YUN FU, XIAO HU, CHEE-YOON YUE
Polymer and Polymer Composites Group, Advanced Materials Research Centre, Nanyang Technological University, Singapore 639798, Republic of Singapore
E-mail: assyfu@ntu.edu.sg

In this paper a new micromechanical model for predicting the transverse modulus of unidirectional continuous and discontinuous fiber composites is proposed. This model is based on modeling a composite with a regular array of volume elements and constructing a stress pattern based on simple averaging procedures in the direction transverse to the fiber axis for a representative volume element. The effects of fiber aspect ratio, interfiber spacing and fiber end gap on the transverse modulus of discontinuous fiber composites are discussed in detail. The predictions of the model are compared with existing experimental results for various fiber/matrix systems and very good agreement is found. The present model has advantages over other existing models not only because the effects of fiber aspect ratio, interfiber spacing and fiber end gap are taken into account and the expression for the transverse modulus of composites is simple in form but also because the present model gives precise predictions of the transverse composite modulus.

1. Introduction

The prediction of the transverse modulus (E_{cy}) of unidirectional fiber composites is of great importance not only because the transverse modulus itself is one important property of engineering materials but also because it is used as an elastic constant in predicting the stiffness of general laminates or the off-axis stiffness of unidirectional laminates [1] and the stiffness of short-fiber-reinforced composites [2–4]. The theoretical expression for E_{cy} must be simple in form in order to use it conveniently as an elastic constant in the prediction of the stiffness of general laminates [1] or short-fiber composites [2–4]. There is large body of work on models that predict the transverse modulus of unidirectional fiber composites in terms of the properties of the constituents. The models can be classified into two categories according to whether the transverse composite modulus depends on fiber aspect ratio.

Most of the existing models assumed that the transverse composite modulus (E_{cy}) was independent of fiber length-to-diameter ratio. The inverse Rule-of-Mixtures (iRoM) equation [1, 5, 6] (i.e. the constant stress model [7]) for E_{cy} was derived by assuming that the fibers have a rectangular cross-section and employing the Rules-of-Mixtures for the strains of the composite and its constituents. The iRoM equation was modified by considering the constitutive relations of the constituents [1]. The advantage of the two models is that they are simple in form and thus convenient to use, but they were not satisfactorily applied to experimental results [1]. The Halpin-Tsai equation [8–10] was derived using a semi-empirical approach [8–10]. The Halpin-Tsai equation has been widely cited in the literature because it provides a fairly good prediction of E_{cy} for continuous fiber composites. Shaffer [11] derived two equations for the transverse composite modulus using the mechanics of materials method. One of these equations is applicable when fiber volume fraction is less than 68% and the other when fiber volume fraction is greater than 68%. Both equations predict low values when compared with experiment. Paul [12] derived bounds for E_{cy} by treating the composite as being transversely isotropic. Paul's bounds are too far apart to be of much practical utility. Tsai [13] considered the problem of parallel elastic cylindrical inclusions in an elastic matrix and derived upper and lower bounds for E_{cy} by interchanging the role of fiber and matrix in the potential energy theorem. Since the bounds are far apart, Tsai hypothesized that the transverse composite modulus lies somewhere between the two bounds. Hashin and Rosen [14] considered both hexagonal and random arrays of fibers. They used potential and complementary energy theorems to derive two bounds for E_{cy}. The bounds obtained by Hashin and Rosen are much improved. Numerical solution techniques have also been used to evaluate the transverse composite modulus. Adams and Doner [15] used the finite difference method to predict the transverse modulus of continuous fiber composites. Chen and Lin [16] and Theocaris *et al.* [17] employed the finite-element method for the purpose. Although numerical modeling of the transverse composite modulus is in principle possible, the effort required for its realization is high, namely time-consuming and high cost.

The above models are only suitable for continuous fiber composites since they neglected the effect of fiber aspect ratio. Some other models considered the effect of fiber aspect ratio. The self-consistent approach, namely the method of Hill [18, 19], was adopted to derive the transverse modulus of unidirectional short fiber composites [20, 21]. The model considered the dependence of E_{cy} on fiber aspect ratio. However, the final expression is given as a function of longitudinal modulus, bulk modulus, shear modulus and Poisson's ratio. Thus, it is not convenient to use the expression to predict E_{cy}. Also, the cell-stress approach was employed by Chen and Cheng [22] to derive the transverse modulus of short fiber composites. But their final expression for E_{cy} is quite complicated and hence is not convenient to use and its predictions were not compared with any experimental results. The effects of fiber aspect ratio, interfiber spacing and fiber end gap on the transverse composite modulus could be derived in principle but were not studied possibly due to the complexity of the expression for E_{cy}. It will be demonstrated in the present study that the Chen-Cheng expression gives an underestimation of the transverse composite modulus. Moreover, Whitney [23] proposed a model for the transverse modulus for unidirectional short composites by modifying the three-phase embedded concentric cylinder model [24]. The fiber and matrix are represented as concentric cylinders. However, the theory was not compared with either other theories or experimental results and hence its validity was not examined.

In this paper, we develop a new micromechanical model for predicting the transverse modulus of unidirectional continuous and discontinuous fiber composites, which is based on modeling a composite with a regular array of volume elements, constructing a stress pattern using simple averaging approaches for a representative volume element in the direction transverse to the fiber axis. With the present model the effects of fiber aspect ratio, interfiber spacing and fiber end gap on the transverse modulus of discontinuous composites are discussed in detail. The present model is compared with some existing experimental results for various fiber/matrix systems. In addition, the present model is compared with other models and the advantages of the present model are demonstrated.

2. Theory

Consider a rectangular specimen with lengths of c_1, c_2 and c_3 (the c_3 axis is parallel to the fiber axis or the x axis) as shown in Fig. 1. It is assumed that the fibers in the unidirectional fiber composite are distributed uniformly in the matrix and the fiber/matrix interfacial adhesion is perfect (only if the fiber/matrix interfacial adhesion is good enough, the interfacial adhesion has little influence on transverse composite modulus since E_{cy} is a property of material at low strain). The case

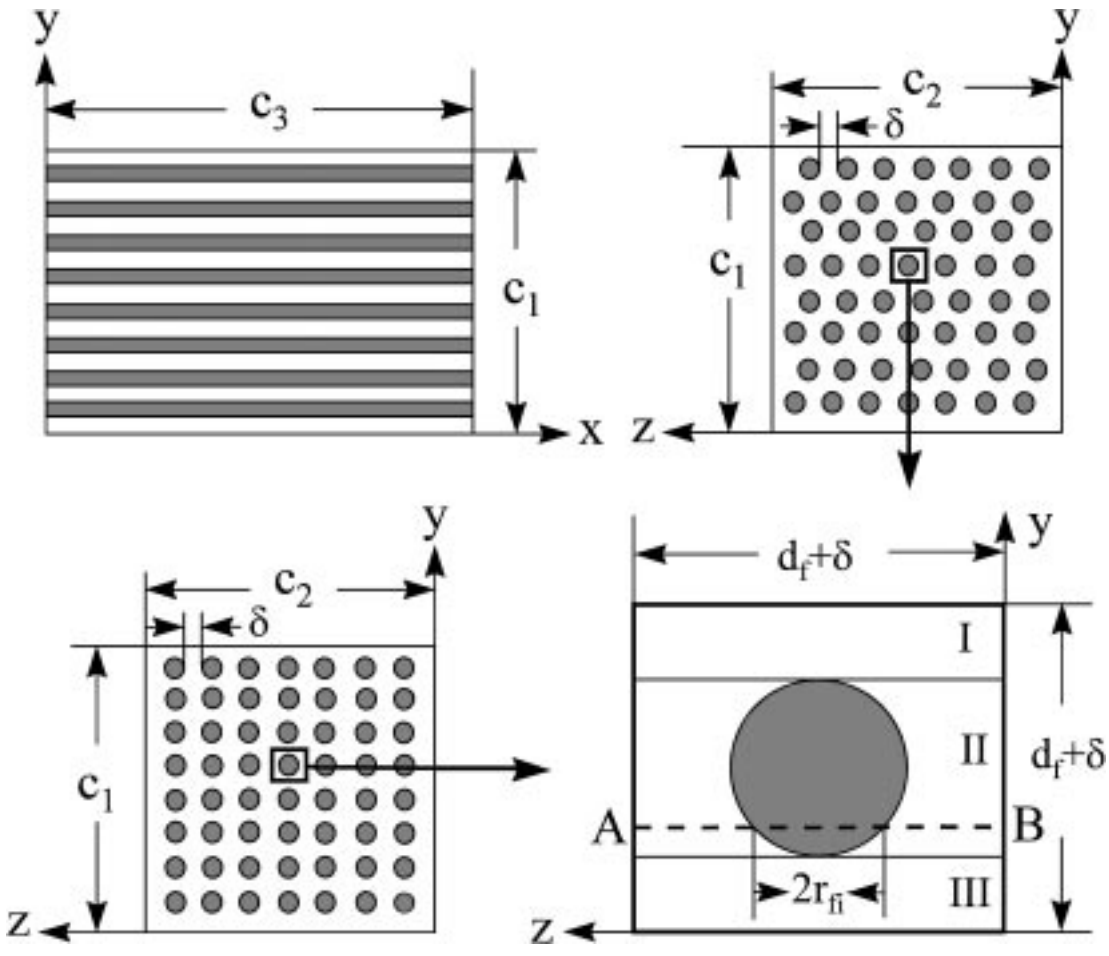

Figure 1 Schematic drawing of a continuous fiber composite and a corresponding simple representative volume element. A perfect bond is assumed between the fiber and the matrix.

of continuous fibers will be considered first. For both square and hexagonal arrangements of fibers, a representative volume element can be chosen as shown in Fig. 1. The representative volume element can be divided into three regions: I, II and III along the x-z plane as shown in Fig. 1. In regions I and III, the matrix bears the load alone and hence the mean matrix strain $\bar{\varepsilon}_{my}$ can be supposed to be approximately equal to:

$$\bar{\varepsilon}_{my} = \sigma_y / E_m \tag{1}$$

where σ_y is the applied stress in the y direction and E_m the matrix modulus.

In any given cross-section ABB′A′ of region II parallel to the x-z plane (where the line A′B′ not shown in Fig. 1 is parallel to the line AB), the stress equilibrium condition can be written as follows:

$$\frac{2r_{fi}}{d_f + \delta}\sigma_{fy} + \frac{d_f + \delta - 2r_{fi}}{d_f + \delta}\sigma_{my} = \sigma_y \tag{2}$$

where σ_{fy} and σ_{my} are the transverse fiber stress and the transverse matrix stress, respectively. d_f is the fiber diameter, δ the interfiber spacing and $2r_{fi}$ the string length of the fiber cross section intersecting with the cross-section ABB′A′.

In region II, both the matrix and the fiber bear the load. In the given cross-section ABB′A′, the matrix strain must be the same as the fiber strain since the fiber/matrix interface is assumed to be perfect (i.e. the fiber is completely bonded with the matrix), otherwise the fiber would debond from the matrix. Thus, Equation 2 becomes:

$$\frac{2r_{fi}}{d_f + \delta}E_{fy}\varepsilon_{fy} + \frac{d_f + \delta - 2r_{fi}}{d_f + \delta}E_m\varepsilon_{fy} = \sigma_y \tag{3}$$

where E_{fy} is the transverse fiber modulus and ε_{fy} the transverse fiber strain.

We now estimate the mean transverse fiber strain $\bar{\varepsilon}_{fy}$. First, we need to evaluate the mean value of r_{fi}, namely, $\bar{r}_{fi}$. Assume the fiber diameter is uniformly divided into n segments (n is very large), the length of each segment is then equal to $2r_f/n$ (r_f is the fiber radius). Thus

$$\frac{2r_f}{n}\sum_{i=1}^{n} 2r_{fi} = \pi r_f^2 \tag{4}$$

and

$$\bar{r}_{fi} = \frac{\sum_{i=1}^{n} r_{fi}}{n} = \frac{\pi}{4}r_f \tag{5}$$

Replacing r_{fi} with $\bar{r}_{fi}$ and ε_{fy} with $\bar{\varepsilon}_{fy}$ in Equation 3 gives:

$$\frac{2\bar{r}_{fi}}{d_f + \delta}E_{fy}\bar{\varepsilon}_{fy} + \frac{d_f + \delta - 2\bar{r}_{fi}}{d_f + \delta}E_m\bar{\varepsilon}_{fy} = \sigma_y \tag{6}$$

In addition, we suppose that $c_1 = m_1(d_f + \delta)$ and $c_2 = m_2(d_f + \delta)$, where m_1 and m_2 are integers. Thus, there are $m_1 \times m_2$ representative volume elements in the composite. The fiber volume fraction can be obtained as:

$$v_f = \frac{\pi r_f^2}{(d_f + \delta)^2} \tag{7}$$

Equations 5–7 can be combined to give the mean transverse fiber strain:

$$\bar{\varepsilon}_{fy} = \frac{\sigma_y}{\sqrt{\frac{\pi v_f}{4}}E_{fy} + \left(1 - \sqrt{\frac{\pi v_f}{4}}\right)E_m} \tag{8}$$

Therefore, the composite strain ε_{cy} is given by

$$\begin{aligned}\varepsilon_{cy} &= v_{\mathrm{II}}\bar{\varepsilon}_{fy} + (v_{\mathrm{I}} - v_{\mathrm{III}})\bar{\varepsilon}_{my} \\ &= \frac{d_f}{d_f + \delta}\bar{\varepsilon}_{fy} + \frac{\delta}{d_f + \delta}\bar{\varepsilon}_{my}\end{aligned} \tag{9}$$

where v_{I}, v_{II} and v_{III} are the volume fractions of regions I, II and III, respectively. Consequently, by inserting Equations 1, 7 and 8 into Equation 9, we obtain

$$\begin{aligned}\varepsilon_{cy} = \sqrt{\frac{4v_f}{\pi}}&\frac{\sigma_y}{\sqrt{\frac{\pi v_f}{4}}E_{fy} + \left(1 - \sqrt{\frac{\pi v_f}{4}}\right)E_m} \\ &+\left(1 - \sqrt{\frac{4v_f}{\pi}}\right)\frac{\sigma_y}{E_m}\end{aligned} \tag{10}$$

Since $\varepsilon_{cy} = \sigma_y / E_{cy}$, the transverse composite modulus E_{cy} follows immediately from Equation 10:

$$\begin{aligned}\frac{1}{E_{cy}} = &\frac{\sqrt{4v_f/\pi}}{\sqrt{\pi v_f/4}E_{fy} + \left(1 - \sqrt{\pi v_f/4}\right)E_m} \\ &+\frac{\left(1 - \sqrt{4v_f/\pi}\right)}{E_m}\end{aligned} \tag{11}$$

Equation 11 gives the transverse modulus of unidirectional continuous fiber composites. An expression for the transverse modulus of discontinuous fiber composites is now developed.

Assume that fibers of a length L_f are distributed uniformly in the composite, and the interfibre spacing is δ and the gap between two end-to-end fibers is L_1. A representative volume element is arbitrarily chosen as shown in Fig. 2. The fiber volume fraction is then

$$\begin{aligned}v_f &= \frac{\pi r_f^2 L_f}{(2r_f + \delta)^2(L_f + L_1)} \\ &= \frac{\pi}{4(1 + \delta/d_f)^2(1 + L_1/L_f)}\end{aligned} \tag{12}$$

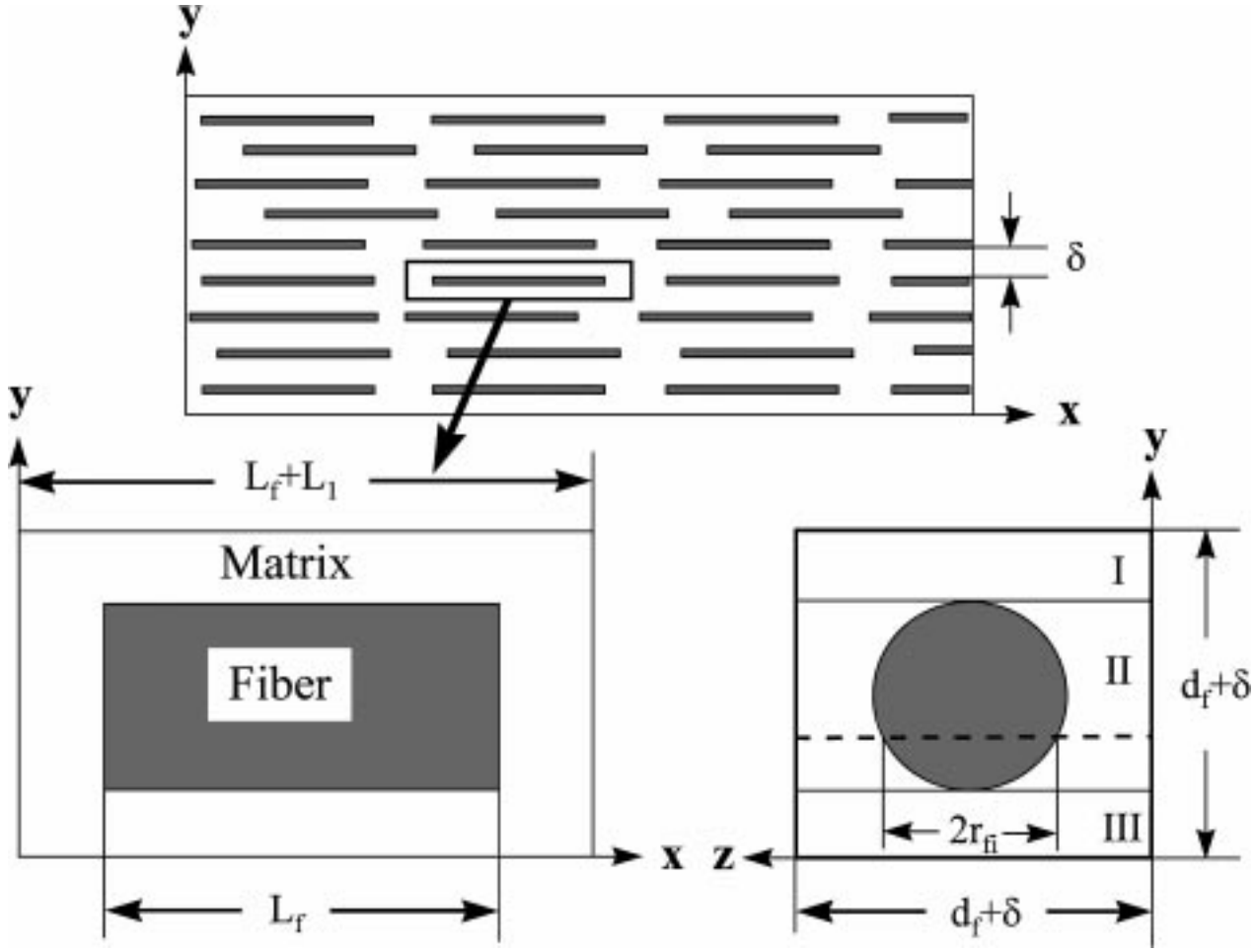

Figure 2 Schematic drawing of a discontinuous fiber composite and a corresponding simple representative volume element. A perfect bond is assumed between the fiber and the matrix.

Using the same treatment as for the case of continuous fibers, we divide the cross section of the element into three regions parallel to the *x*-*z* plane as shown in Fig. 2. In regions I and III, the matrix bears load alone, then the mean matrix strain is the same as expressed in Equation 1.

In region II, both the fiber and the matrix bear the load and their strains in this region should be approximately the same. The stress equilibrium equation in the cross-section parallel to the *x*-*z* plane denoted by the dotted line can be written as follows:

$$\frac{2r_{fi}L_f}{(d_f+\delta)(L_f+L_1)}E_{fy}\varepsilon_{fy} + \left[1-\frac{2r_{fi}L_f}{(d_f+\delta)(L_f+L_1)}\right]E_m\varepsilon_{fy}=\sigma_y \quad (13)$$

By replacing $2r_{fi}$ with $2\bar{r}_{fi}$ and ε_{fy} with $\bar{\varepsilon}_{fy}$ in Equation 13 and combining with Equation 12, then we get the mean transverse fiber strain

$$\bar{\varepsilon}_{fy}=\frac{\sigma_y}{\sqrt{\frac{\pi v_f}{4(1+L_1/L_f)}}E_{fy}+\left(1-\sqrt{\frac{\pi v_f}{4(1+L_1/L_f)}}\right)E_m} \quad (14)$$

The composite strain is then given by

$$\varepsilon_{cy}=\frac{d_f}{d_f+\delta}\bar{\varepsilon}_{fy}+\frac{\delta}{d_f+\delta}\bar{\varepsilon}_{my} \quad (15)$$

By inserting Equations 1, 12 and 14 into Equation 15 and using the relationship: $\varepsilon_{cy}=\sigma_y/E_{cy}$, we obtain

$$\frac{1}{E_{cy}}=\frac{\sqrt{4v_f(1+L_1/L_f)/\pi}}{\sqrt{\pi v_f/[4(1+L_1/L_f)]}E_{fy}+\left(1-\sqrt{\pi v_f/[4(1+L_1/L_f)]}\right)E_m}+\frac{\left(1-\sqrt{4v_f(1+L_1/L_f)/\pi}\right)}{E_m} \quad (16)$$

In the limit of $L_1/L_f = 0$, the transverse modulus of discontinuous fiber composites becomes independent of the fiber length (or fiber aspect ratio) and Equation 16 reduces to Equation 11.

3. Results and discussion

The following data are used for the parameters, except where noted otherwise: $E_{fy} = 72.4$ GPa, $E_m = 2.1$ GPa, $L_1 = 10$ μm, $L_f = 1000$ μm, $d_f = 10$ μm and $v_f = 0.50$. The transverse composite modulus is evaluated based on Equations 12 and 16. The effects of fiber aspect ratio, interfiber spacing and fiber-end-gap on the transverse modulus of discontinuous fiber composites are discussed in detail in the following.

Fig. 3 exhibits the effects of fiber aspect ratio and interfiber spacing on the transverse modulus of discontinuous fiber composites. It can be seen from Fig. 3a that the transverse composite modulus decreases rapidly with the increase of fiber aspect ratio when it is small (e.g. < 100) whereas it decreases slowly with increasing fiber aspect ratio and becomes insensitive to the fiber aspect ratio when it is large (e.g. > 100). This is because increasing the fiber length decreases the number of fiber ends and thus the amount of matrix between fiber ends. Since the amount of matrix is fixed, it moves towards the space between the fibers and increases the interfiber spacing and thus decreases the transverse composite modulus. Consequently, it is observed in Fig. 3b that the interfiber spacing increases rapidly with increase of fiber aspect ratio when it is small (e.g. < 100) but increases slowly with fiber aspect ratio and eventually becomes insensitive to it when it is large (e.g. > 100). The transverse composite modulus decreases almost linearly with increase of interfiber spacing (Fig. 3c).

Fig. 4 reveals the effect of fiber end gap on the transverse modulus of composites. Since the interfiber spacing decreases almost linearly with increase of fiber end gap (see Fig. 4a) and the transverse composite modulus decreases with increase of interfiber spacing as shown in Fig. 3c, it is observed that the transverse modulus of composites increases almost linearly with increase of fiber end gap (see Fig. 4b).

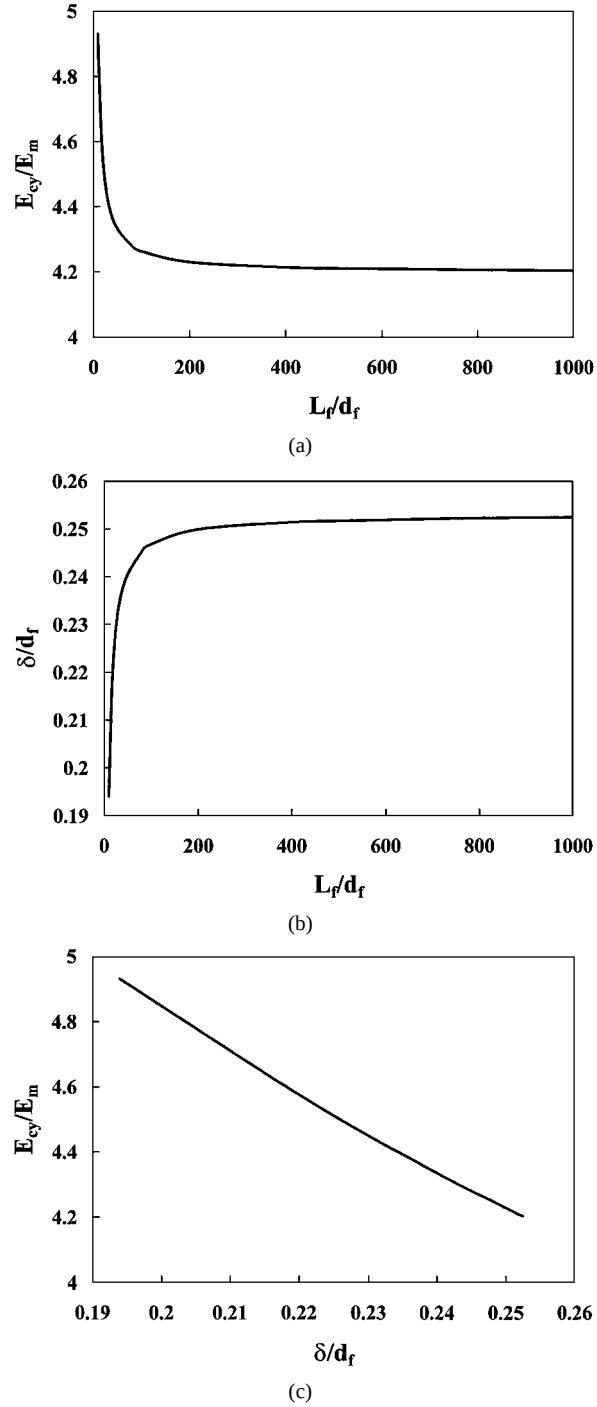

Figure 3 Effects of fiber aspect ratio and interfiber spacing on the transverse modulus of discontinuous fiber composites: (a) E_{cy}/E_m vs L_f/d_f (b) δ/d_f vs L_f/d_f and (c) E_{cy}/E_m vs δ/d_f.

4. Application and comparison

We now compare predictions using Equation 16 with some existing experimental results [1, 25, 26] together with predictions of the iRoM Equation [1, 5–7] and its modified version [1], the Halpin-Tsai Equation [8–10], the self-consistent theory [20, 21], the Chen-Cheng theory (i.e. the cell-stress approach) [22] and the Whitney theory [23].

The iRoM Equation is [1, 5–7]:

$$\frac{1}{E_{cy}} = \frac{v_f}{E_{fy}} + \frac{v_m}{E_m} \tag{17}$$

The modified iRoM (miRoM) Equation is [1]:

$$\frac{1}{E_{cy}} = \frac{v_f}{E_{fy}} + \frac{v_m}{E_m} - v_f v_m \frac{v_f^2 E_m/E_{fy} + v_m^2 E_{fy}/E_m - 2v_f v_m}{v_f E_{fy} + v_m E_m} \tag{18}$$

The Halpin-Tsai Equation [8–10] can be written as follows:

$$E_{cy} = E_m(1 + 2\alpha v_f)/(1 - \alpha v_f) \tag{19}$$

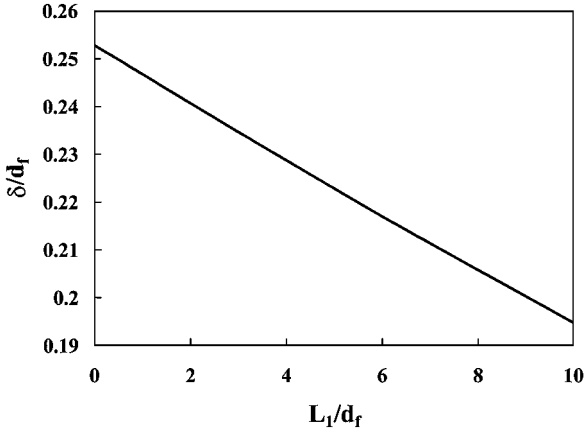

(a)

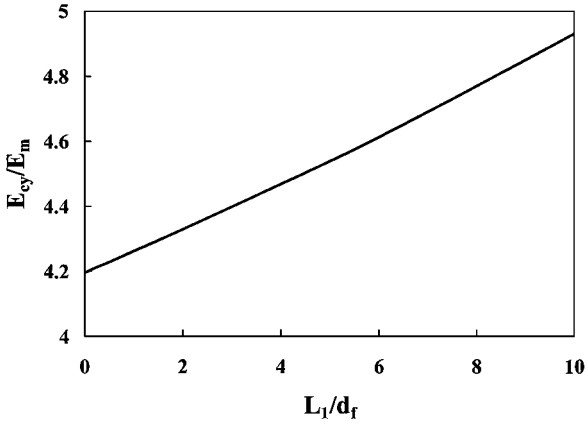

(b)

Figure 4 Effect of fiber end gap on the transverse modulus of discontinuous fiber composites: (a) δ/d_f vs L_1/d_f and (b) E_{cy}/E_m vs L_1/d_f.

where

$$\alpha = (E_{fy}/E_m - 1)/(E_{fy}/E_m + 2) \qquad (20)$$

In Equations 17–20 the subscript y is used to denote the transverse modulus of fibers for the case of transversely isotropic fibers.

Equation 16 and the first three models above (Equations 17–19) are applied to some existing experimental results for continuous, discontinuous and particulate glass/epoxy composites (continuous and particulate composites are the two limiting cases of discontinuous fiber composites) [25]. The results are listed in Table I, where particular values of the parameters are $E_{fy} = 72.4$ GPa, $E_m = 2.1$–2.8 GPa, $\nu_f = 0.22$, $\nu_m = 0.35$ and $v_f = 0.5$ (for short glass fibers and glass beads) and 0.6 (for continuous glass fibers) [25]. For the case of short-fibers, $L_1/L_f = 0.02$ was used. The theoretical values of the transverse modulus (assuming $L_1 = \delta$ and $L_f = d_f = 10$ μm) are also given in order to compare the present theory with the experimental results for particulate composites. Table I shows that the theoretical results predicted by Equation 16 agree very well with the experimental results for the two cases of continuous and discontinuous fibers. For the particulate composite, the predicted values of the transverse modulus by this theory are reasonably close to the experimental results. The difference in the latter can probably be attributed to the fact that the fibers with an aspect ratio of one are cylindrical in shape and not normal particles. The results predicted by the Halpin-Tsai Equation (Equation 19) are approximately consistent with but somewhat lower than the experimental results. However, the iRoM and miRoM (Equations 17 and 18) give much lower predicted values of the transverse composite modulus than those experimentally observed, as reported in [1].

The predictions of the models above are also compared with experimental results for the graphite/epoxy composite system, where the graphite fibers are transversely isotropic and the boron/epoxy composite system, where the boron fibers have a very high modulus [1]. The results are listed in Table II, where particular values for the parameters are $E_{fy} = 16.6$ GPa for graphite fibers, $E_{fy} = 410$ GPa for boron fibers, $E_m = 3.45$ GPa, $\nu_f = 0.2$ for both fibers, $\nu_m = 0.35$ and $v_f = 0.70$ (for graphite fibers) and 0.50 (for boron

TABLE I Application of the present theory and other theories [1, 5, 8–10] to the existing experimental results for some glass/epoxy composites [25]

			Transverse stiffness, E_{cy} (GPa)				
Material	E_m (GPa)	v_f	Experimental results	Halpin-Tsai equation	iRoM equation	miRoM equation	The present model
Glass bead/epoxy	2.1	0.5	10.3	—	—	—	11.56
	2.8	0.5	11.7	—	—	—	14.33
Short glass fiber/epoxy	2.1	0.5	9.6	7.44	4.08	4.59	9.09
Continuous glass fiber/epoxy	2.1	0.6	12.4	9.82	5.03	5.66	12.95
	2.8	0.6	14.5	12.48	6.62	7.41	16.07

TABLE II Application of the present theory and other theories [1, 5, 8–10] to the existing experimental results for a graphite/epoxy composite and a boron/epoxy composite [1]

		Transverse stiffness, E_{cy} (GPa)				
Material	v_f	Experimental results	Halpin-Tsai equation	iRoM equation	miRoM equation	The present model
Graphite/epoxy	0.70	10.3	10.11	7.74	8.21	11.40
Boron/epoxy	0.50	18.5	13.29	6.84	7.77	16.23

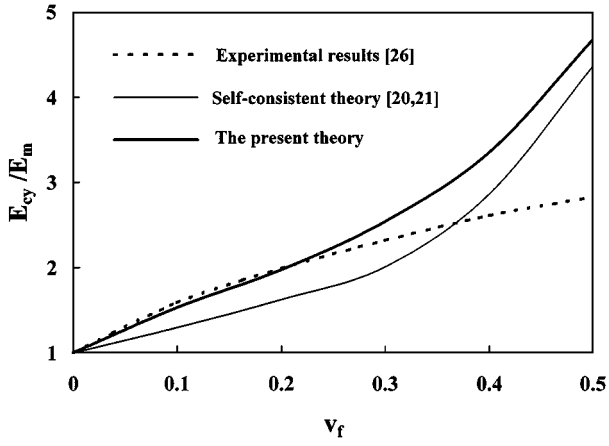

Figure 5 Comparison of the present theory with the self-consistent theory [20, 21] and experimental results [26] for a nylon 12-PRD49 system with $L_f/d_f = 882$ and $E_f/E_m = 105$.

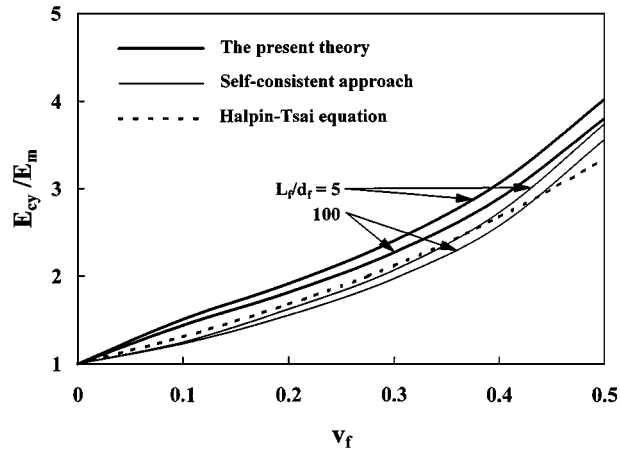

Figure 6 Comparison of the present theory with the self-consistent theory [20, 21] and the Halpin-Tsai equation [8–10] in the predictions of the transverse composite modulus as a function of fiber volume fraction, where $L_f/d_f = 5$ and 100, $E_f/E_m = 20$, $v_f = 0.3$ and $v_m = 0.35$.

fibers) [1]. Table II reveals that for the graphite/epoxy system the present theory and the Halpin-Tsai theory are in good agreement with the experimental result while the iRoM and its modified version provide lower predicted values than the experimental one. For the boron/epoxy system, the present theory provides a better prediction than all other three theories which give much lower values than the experimental result.

Fig. 5 depicts the comparison of the present theory with the self-consistent theory [20, 21] and the experiments [26] on the transverse modulus for a nylon 12-PRD49 composite system where $E_f/E_m = 105$ and $L_f/d_f = 882$. A uniform fiber distribution i.e. $L_1 = \delta$ is assumed. At low fiber volume fractions, the present theory agrees very well with the experimental results but the predicted values with the self-consistent theory are lower than the experimental values. At high fiber volume fractions the theoretical values are higher than the experimental ones. For the present theory, the discrepancy may be attributed to the fact that the value of fiber end gap (L_1) used may be greater than the real value since the ends of fibers are closer to each other as v_f increases. A greater value of L_1 would lead to a higher prediction of the transverse composite modulus.

The comparison of the present theory with the self-consistent theory [20, 21] and the Halpin-Tsai equation [8–10] is further made in Fig. 6, where $E_f/E_m = 20$, $v_f = 0.3$ and $v_m = 0.35$. The predicted values by the present theory are somewhat higher than those predicted by the self-consistent theory [20, 21]. At low v_f, the predicted values by the Halpin-Tsai equation [8–10] lie between those predicted by the other two theories; at high v_f, the predicted values by the Halpin-Tsai equation are lower than those predicted by the other two theories.

The comparison of the present theory with the Chen-Cheng theory (cell-stress model) [22] and the Halpin-Tsai equation [8–10] is made in Fig. 7, where $E_f/E_m = 21.19$, $L_f/d_f = 20$ and $L_1/L_f = 0.05$. Fig. 7 shows that the values of the transverse composite modulus predicted by the present theory are higher than those by the other two theories and the predicted values by the Chen-Cheng theory are lower than those predicted by the Halpin-Tsai Equation which is for continuous fiber composites. However, it has been clearly shown in the present study and also in the self-consistent theory [20, 21] and the Whitney theory [23] that the transverse modulus of a unidirectional short-fiber composite is higher than that of a corresponding continuous fiber composite since E_{cy} decreases with fiber length, and the Halpin-Tsai Equation has been well recognized to give good predictions for continuous fiber composites or somewhat lower predictions for some short-fiber composites, therefore the Chen-Cheng theory would underestimate the transverse modulus of unidirectional discontinuous fiber composites. Moreover, the effects of interfiber spacing and fiber end gap on the transverse composite modulus were not studied using the Chen-Cheng theory, possibly because their expression for E_{cy} is too complicated to use.

Fig. 8 shows the comparison of the present theory with the Whitney theory [23] and the Halpin-Tsai equation [8–10], where $E_f/E_m = 70$, $v_f = 0.4$ and $L_1/\delta = 1$ (uniform fiber distribution). Fig. 8 shows that the predicted values of E_{cy} by the present theory are higher than those predicted by the Whitney theory [23]. The

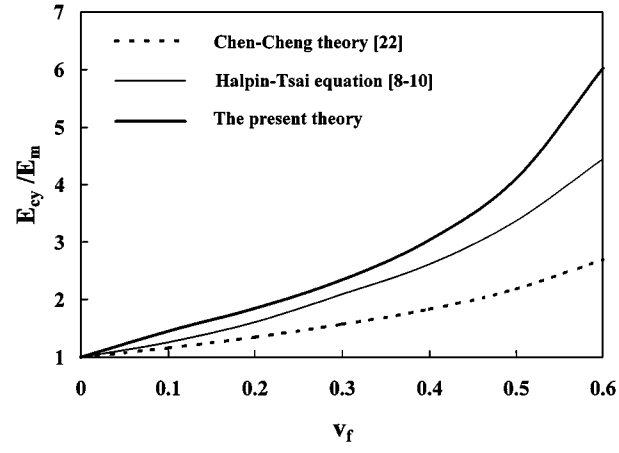

Figure 7 Comparison of the present theory with the Chen-Cheng theory [22] and the Halpin-Tsai equation [8–10], where $L_f/d_f = 20$, $L_1/d_f = 0.05$ and $E_f/E_m = 21.19$.

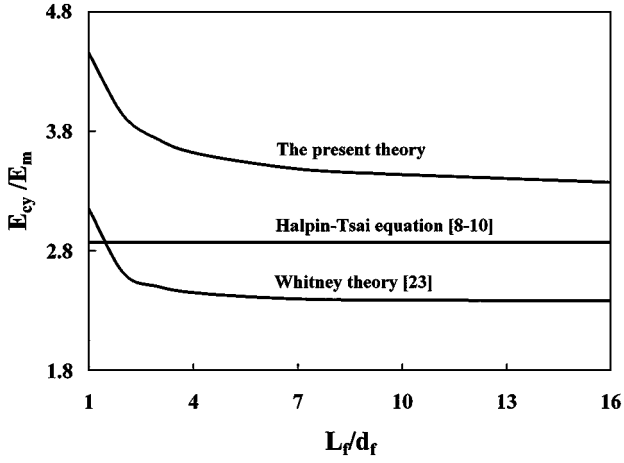

Figure 8 Comparison of the present theory with the Whitney theory [23] and the Halpin-Tsai equation [8–10], where $E_f/E_m = 70$, $v_f = 0.4$ and $L_1/\delta = 1$ (uniform fiber distribution).

values predicted by the Halpin-Tsai equation [8–10] lie between those predicted by other two theories except at $L_f/d_f <$ about 1.5. Since the Halpin-Tsai Equation is for continuous fiber composites and the transverse composite modulus of continuous composites should be higher than that of discontinuous fiber composites, then the Whitney theory would give lower predictions of E_{cy} for discontinuous composites.

In conclusion, the present model for the transverse modulus of unidirectional fiber composites has some advantages over other models not only because the present model considers the effects of fiber aspect ratio, interfiber spacing and fiber end gap and the expression for E_{cy} is simple in form and hence easy to use but also because it gives precise predictions of the transverse composite modulus for various fiber/matrix systems.

5. Conclusions

In the present study, a new micromechanical model has been developed for the transverse modulus of unidirectional continuous and discontinuous fiber composites. It has been shown that the transverse modulus of discontinuous fiber composites decreases rapidly with the increase of fiber aspect ratio when the fiber aspect ratio is small while the transverse modulus is insensitive to the fiber aspect ratio when the fiber aspect ratio is large. Moreover, the transverse modulus of discontinuous composites increases with the decrease of interfiber spacing and the increase of fiber end gap. The present model has been revealed to give reliable predictions of the transverse composite modulus for various fiber/matrix systems. The comparison of this model with other models and experiments has demonstrated that the present model has some advantages over other theories.

Acknowledgements

The kind reading and comments of this paper by Prof. Yiu-Wing Mai, the Director of Centre for Advanced Materials Technology, Dept. of Mechanical & Mechatronic Engineering, the University of Sydney, Australia are gratefully acknowledged.

References

1. S. W. TSAI and H. T. HAHN, "Introduction to Composite Materials" (Technomic Publ. Co., Lancaster, PA, 1980).
2. S. Y. FU and B. LAUKE, *Compos. Sci. Technol.* **58** (1998) 389.
3. Z. YU, J. BRISSON and A. AIT-KADI, *Polym. Compos.* **15** (1994) 64.
4. M. XIA, H. HAMADA and Z. MAEKAWA, *Int. Polym. Process.* **10** (1995) 74.
5. M. R. PIGGOTT, in "Load-Bearing Fiber Composites" (Pergamon Press Ltd., Oxford, 1980) p. 69.
6. M. R. BADER and A. R. HILL, in "Materials Science and Technology: A Comprehensive Treatment," Vol. 13, edited by R. W. Cahn, P. Haasen and E. J. Kramer (VCH Verlagsgesellschaft mbH, Weinheim, Germany and VCH Publishers Inc., New York, 1993) Chap. 7, pp. 291–338.
7. B. D. AGARWAL and L. J. BROUTMAN, in "Analysis and Performance of Fiber Composites" (Wiley-Interscience, New York, 1990) p. 72.
8. J. C. HALPIN and S. W. TSAI, U.S. Air Force Materials Laboratory Rept, AFML TR 67–423 (1967).
9. J. C. HALPIN, *J. Compos. Mater.* **3** (1969) 732.
10. J. C. HALPIN and J. L. KARDOS, *Polym. Engin. Sci.* **16** (1976) 344.
11. B. W. SHAFFER, *J. AIAA* **2** (1964) 348.
12. B. PAUL, *Trans. Metall. Soc. AIME* **218** (1960) 36.
13. S. W. TSAI, NASA CR-71 (1964).
14. Z. HASHIN and B. W. ROSEN, *J. Appl. Mechanics, Trans. ASME* **31** (1964) 223.
15. D. F. ADAMS and D. R. DONER, *J. Compos. Mater.* **1** (1967) 152.
16. P. E. CHEN and J. M. LIN, *Mater. Res. Stand., MTRSA* **9** (1969) 29.
17. P. S. THEOCARIS, G. E. STAVROULAKIS and P. D. PANAGIOTOPOULOS, *Compos. Sci. Technol.* **57** (1997) 573.
18. R. HILL, *J. Mech. Phys. Solids* **13** (1965)189.
19. R. HILL, *ibid.* **13** (1965)213.
20. T. W. CHOU, S. NOMURA and M. TAYA, *J. Compos. Mater.* **14** (1980) 178.
21. T. W. CHOU, S. NOMURA and M. TAYA, Modern Developments in Composite Materials and Structures, the Winter Annual Meeting of the American Society of Mechanical Engineers, New York, December 2–7, 1979, edited by J. R. Vinson (ASME, New York, 1979) pp. 149–164.
22. D. CHEN and S. CHENG, *J. Reinf. Plast. Compos.* **14** (1995) 333.
23. J. M. WHITNEY, *J. Reinf. Plast. Compos.* **16** (1997) 714.
24. R. M. CHRISTENSEN, "Mechanics of Composite Materials" (Wiley-Interscience, New York, 1979).
25. L. KARDOS, in "International Encyclopedia of Composites," Vol. 5, edited by S. M. Lee (VCH Publishers, New York, 1991) pp. 130–141.
26. B. F. BLUMENTRITT, B. T. VU and S. L. COOPER, *Polym. Engin. Sci.* **8** (1968) 186.

Received 17 September 1998
and accepted 18 September 1998